J Therm Anal Calorim (2012) 109:825–829
DOI 10.1007/s10973-011-1791-3

On the influence of the milling time in the Curie temperature of $Fe_{56}Co_7Ni_7Zr_{10}B_{20}$ investigated by magnetic thermogravimetric analysis

G. F. Barbosa · F. L. A. Machado · A. R. Rodrigues · W. M. Azevedo

Received: 9 May 2011 / Accepted: 6 July 2011 / Published online: 19 July 2011

Abstract Magnetic thermogravimetric analysis (TGM) was used to investigate the influence of the milling time (t_{mill}) in the Curie temperature (T_C) of nanocrystalline powders and of a melt-spun amorphous ribbon with composition $Fe_{56}Co_7Ni_7Zr_{10}B_{20}$. The TGM analysis was carried in a continuous flow of 99.99% pure argon from room temperature up to 1250 K. A magnetic field of 100 Oe was applied throughout the measurements. Nanopowders of $Fe_{56}Co_7Ni_7Zr_{10}B_{20}$ were produced by mechanical alloying the samples in an argon atmosphere for milling times ranging from 1 to 100 h. The samples were characterized by X-ray diffraction and by scanning electron microscopy. The average particle size decreased from 45.4 nm for a powder milled for 1 h to 5 nm after being milled for 100 h. Moreover, T_C (=1126.4 ± 4.4 K) was found to be nearly independent of t_{mill} while for the melt-spun amorphous ribbon it was found to be substantially smaller ($T_C = 482$ K). This is a clear indication that T_C is quite sensitive to the degree of amorphosity present in the sample. The activation energy associated to the crystallization process was estimated from DSC data by using the Kissinger's method to be 193 kJ/mol.

G. F. Barbosa (✉) · F. L. A. Machado · A. R. Rodrigues
Departamento de Física, Universidade Federal de Pernambuco, Recife, PE 50670-901, Brazil
e-mail: gferreira@df.ufpe.br

G. F. Barbosa
Graduate Program in Material Science, Universidade Federal de Pernambuco, Recife, PE 50670-901, Brazil

W. M. Azevedo
Departamento de Química Fundamental, Universidade Federal de Pernambuco, Recife, PE 50670-901, Brazil

Keywords Magnetic thermogravimetry · Nanocrystalline · Amorphous · Magnetic materials

Introduction

Mechanical alloying (MA) was found to be a sample preparation technique which allows one to produce several classes of materials [1]. Essentially, in a MA a precursor powder is continuously fractured and cold welded. This favors a decrease in the average particle size which, in turn, helps the diffusion process and the formation of a desired alloy composition. It is also possible to produce amorphous materials by MA but usually it is a somewhat more difficult to synthesize them due to the formation of solid solutions in the first hours of milling [2]. However, multi-components metastable alloys can be produced after long milling time using high energy ball mills [2–4]. In a study by Liu and Chang [5], the thermal stability of a family of alloys with composition $Fe_{70-x-y}Co_xNi_yZr_{10}B_{20}$ obtained by MA was evaluated. They demonstrated that amorphous phases could be formed for a Co-free alloy composition and for alloys with Ni/Co ratios of 1:1 and 1:3. Magnetic thermogravimetric analysis (TGM), on the other side, was shown to be suitable for measuring critical temperatures of magnetic materials [6]. This is particularly important at high temperatures where other techniques are not so easy to be implemented or high applied magnetic fields are required. For instance, TGM has been used to study the magnetic permeability of soft ferromagnetic alloys and to determine their Curie temperatures (T_C) [7], to study the amorphous nanocrystalline transformation [8], and to measure T_C's in nanocrystalline alloys [9]. Moreover, a modified TGM analysis was developed by Luciani et al.

[10] which allows one to measure the magnetic susceptibility using this kind of technique as well.

In this study, the TGM analysis was employed to study the effect of the milling time (t_{mill}) in the Curie temperature (T_C) of a series of nanopowders with composition of $Fe_{56}Co_7Ni_7Zr_{10}B_{20}$. Amorphous ribbons with the same sample composition were also produced but using a melt-spinning technique for comparison. The samples were characterized by X-ray diffraction (XRD) and by scanning electron microscopy (SEM). The thermal stability was investigated using differential scanning calorimetry (DSC).

Experimental procedure

Blended elemental powders of Fe (99.5%, 100 mesh), Co (99.9%, 100 mesh), Zr (99.5%, 100 mesh), Ni (99%, 100 mesh), B (99.7%, 325 mesh) were milled in a Fritsch Pulverysette-5 planetary mill with vials and balls made of stainless steel. The elements were stoichiometrically weighted to yield an alloy with nominal composition of $Fe_{56}Co_7Ni_7Zr_{10}B_{20}$. The milling ball-to-sample weight ratio (MB:MS) was set to 5:1, while the rotation speed was fixed in 300 rpm. The millings were made under an argon atmosphere and t_{mill} was varied in the interval 1–100 h. Small amounts of the milled powder were collected after pre-defined time intervals for structural and thermal analyses. The remained powder is then further milled for another time interval. We believe that this procedure reduces composition variation associated to the preparation of the starting blended powder. An amorphous ribbon with the same nominal composition was prepared using a melt-spinning technique with the copper wheel rotating at a speed of 2800 rpm. The precursor alloy used in the melt-spinning was prepared by melting a pellet made with the starting blended powder in an arc-furnace under an inert atmosphere of argon. The pellet was melt for five times to increase its homogeneity. The powder samples structure and composition were analyzed by XRD using a Bruker–Siemens D5000 diffractometer with Cu-Kα radiation. The full width at a half maximum (FWHM) of the peak corresponding to the α-Fe phase (main solvent element) was used together with Scherrer's formula [11] to determine the average particle size. The instrumental broadening used to correct the peak with of the milled samples was determined from a XRD measurement performed in a powder quartz sample. The average micro-strain introduced by the milling process was also determined as a function of the t_{mill} using Williamson–Hall plots [12]. The morphology of the milled powders was observed using a JEOL 5900 SEM.

The thermal analyses were made using a thermal analyzer Labsys Evo system (made by SETARAM). The thermogravimetric (TG) and the differential-thermal (DTA) analyses and the DSC measurements were made using a Labsys Evo system (by SETARAM) under a continuous flux of 99.995% pure argon passing through the sample-probe space. Crucibles and lids made of alumina and powder samples weighting in the range 20–30 mg were used throughout the measurements. The Curie temperature was determined by applying 100 Oe magnetic field at the sample space, while the sample weight was measured as a function of the temperature (T). The applied magnetic field was generated by a 2-cm thick NdFeB toroidal hard magnet with internal and external diameters of 8.5 and 17.0 cm, respectively. The magnetic force component added to the sample weight while it is in the ferromagnetic phase nearly vanishes at T_C. Baselines were obtained by performing the measurements in the absence of the applied field for correcting the magnetic data. The TGM system was tested by measuring T_C of powders of high purity (99.99%) Ni, Fe, and Co yielding 632, 1043, and 1390 K for the critical temperatures, respectively. These values agree well with the ones reported in the literature [13, 14].

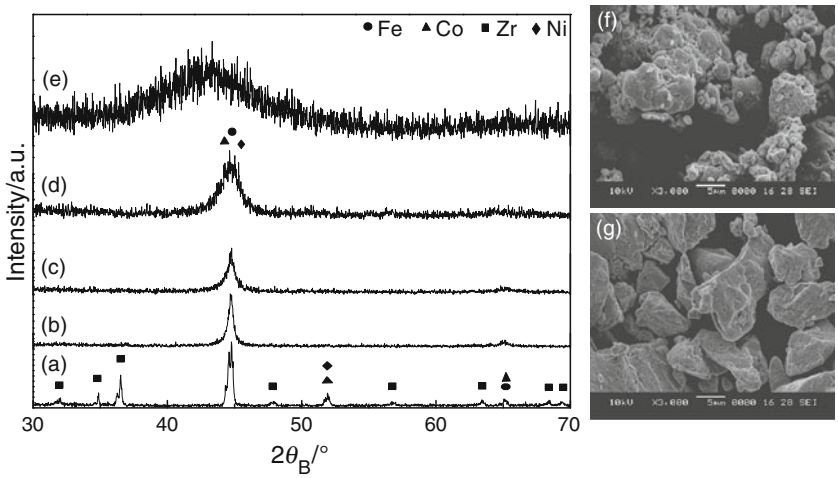

Fig. 1 XRD patterns for as-blended (*a*) and for powder samples of $Fe_{56}Co_7Ni_7Zr_{10}B_{20}$ alloys milled for 10 (*b*), 30 (*c*), and 100 h (*d*) and for an amorphous ribbon with the same sample composition (*e*). Two SEM micrographs for powder samples milled for 1 and 50 h are shown in (*f*) and (*g*), respectively

Experimental results

Representative XRD patterns obtained for the blended and for the as-milled powders for milling times of 10, 30, and 100 h are shown in Fig. 1a–d. For comparison, the pattern for the amorphous ribbons is also shown in Fig. 1e. The spectra were multiplied by different factors to help one to better visualize the relative peak intensities in each of the diffractograms and the increasing in the width of the peaks due to the milling process. It was observed that most intense peak corresponding to the α-Fe (110) component becomes broader while its intensity decreases with increasing milling time. The average crystallite size (D_0) was found to decrease from 45.4 nm for the sample milled for 1 h to 5 nm after milling the sample for 100 h. The average micro-strain (ε) was also obtained. It was found that ε increases monotonically with the milling time. The increasing in ε results mostly from plastic deformations introduced by mechanical collision between the grinding elements (balls and vessel walls) and the powder. The XRD analyses are summarized in Fig. 2. It is important to notice that the powder milled for 100 h has a single broad peak XRD pattern which resembles the one for the amorphous ribbon. The morphology of the particles was investigated by SEM. Two micrographs for powder samples milled for 1 and 50 h are shown in Fig. 1f and g, respectively. They indicate that the morphology evolves from aggregate of small particles to a set of plastic-deformed and flattened grains.

Figure 3 shows DSC data for the powder samples milled for 10, 30, 50, 70, and 100 h. The DSC data were recorded from room temperature to 1273 K in the heating mode at a rate (β) of 0.167 K/s. The indication of T_g, T_x, and T_p in Fig. 3 followed those established by other authors and are in good agreement with the values obtained for material with sample composition close to the ones reported in this study [15, 16]. In order to verify that the samples indeed crystallize above T_x we performed room temperature XRD

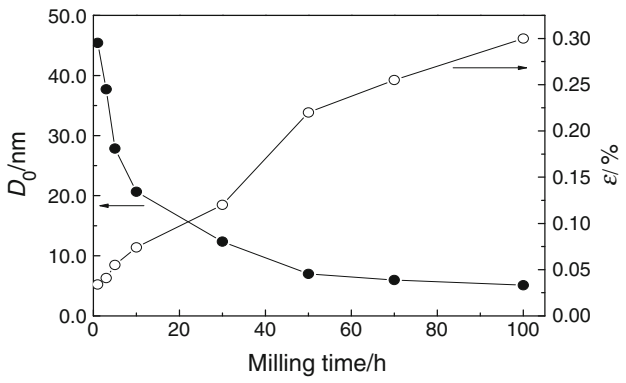

Fig. 2 Average crystallite size (left hand side scale) and average micro-strain (right hand side scale) as function t_{mill} for powder samples of $Fe_{56}Co_7Ni_7Zr_{10}B_{20}$

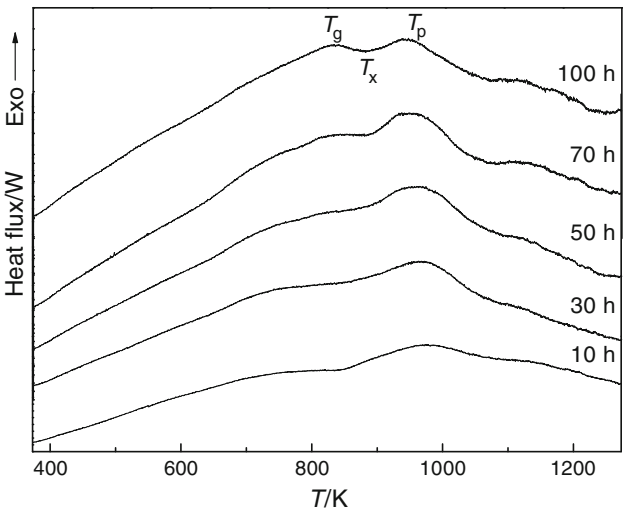

Fig. 3 DSC data for a heating rate β of 0.167 K/s and for powder samples milled for 10, 30, 50, 70, and 100 h

measurements after thermal cycling the samples. The X-rays spectra for a sample milled for 100 h before and after a thermal cycle are shown in Fig. 4a, b. It is important to notice the appearance of several peaks due to the formation of a solid solution in Fig. 4b, while the most intense peak becomes less broader than the corresponding one in Fig. 4a. DSC data for $\beta = 0.133$, 0.167, 0.200, and 0.250 K/s are also presented for the sample milled for 100 h in Fig. 5. This set of curves allows one to determine the glass transition temperature (T_g), the crystallization temperature (T_x), and the crystallization temperature peak (T_p) as a function of the heating rate as shown in Fig. 6. Moreover, the activation energy associated to the crystallization process was estimated to be 193 kJ/mol using the Kissinger's method, e.g., from the slope of a plot of $\ln[\beta/T_p^2]$ versus T_p^{-1} [17]. The TGM data obtained for the milled powder samples yielded values for T_C varying in the

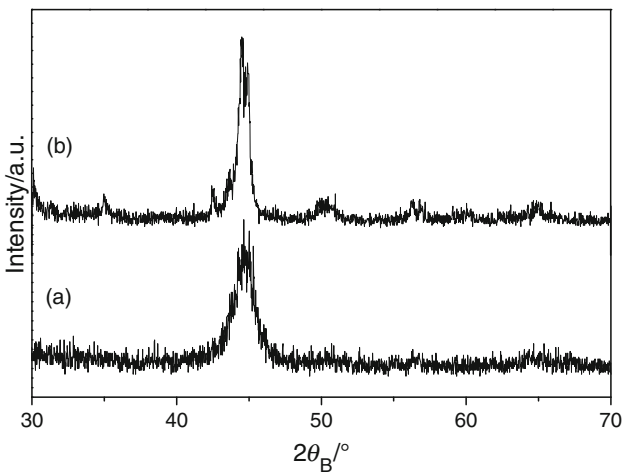

Fig. 4 X-rays spectra for a sample milled for 100 h before (*a*) and after thermal cycling (*b*) the sample at a heating rate of 0.167 K/min

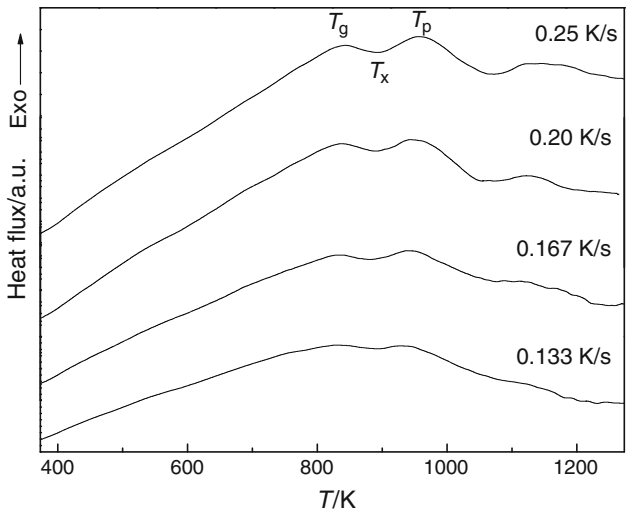

Fig. 5 DSC data for a powder sample of the $Fe_{56}Co_7Ni_7Zr_{10}B_{20}$ alloy milled for 100 h for heating rates β of 0.083, 0.133, 0.167, 0.200, and 0.250 K/s

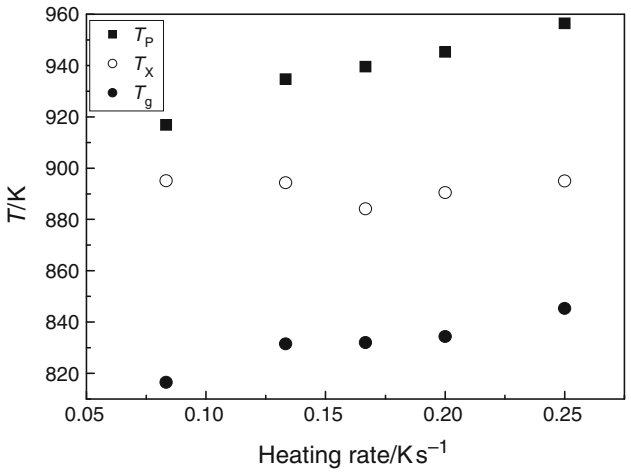

Fig. 6 T_g, T_x, and T_p determined from the DSC data versus the heating rate β for the powder sample milled for 100 h

range 1122.0–1130.8 K. This variation is more likely to be associated to the uncertainty inherent in the determination of T_C plus the error introduced in subtracting the TGM background. However, the Curie temperature for amorphous ribbon was found to be 482 K which is substantially smaller than values for the nanocrystalline powder samples. A TGM set of data for the powder sample milled for 100 h and for a melt-spun amorphous ribbon (inset) is shown in Fig. 7. T_C was measured for different heating rates, but no significant variation was observed. This is a somewhat expected result since T_C is a thermodynamical parameter which depends mainly on the magnetic interaction among spins of nearest neighbors and its dynamics is substantially faster than the structural dynamics.

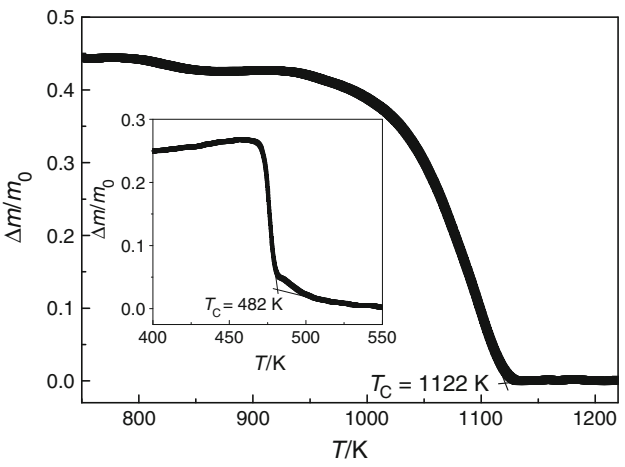

Fig. 7 TGM data for a powder sample of the $Fe_{56}Co_7Ni_7Zr_{10}B_{20}$ alloys milled for 100 h. The *inset* is the TGM data for a melt-spun amorphous ribbon with similar composition

Discussion and conclusions

The XRD data showed that powder milled for 100 h the average particle size becomes quite reduced (5 nm). The XRD diffractogram did also show that the pattern for this sample is essentially made of a quite broad single-peak while a well-defined glass-to-crystalline (T_g) transition temperature was found to be present in the DSC curves. These features are signatures that have been used to assume that the sample is near a transition to an amorphous phase. However, as seen in the XRD spectra for an amorphous sample with the same sample composition the peak for an amorphous phase is significantly broader than the one observed for samples milled for long periods of time. Furthermore, by measuring T_C as a function of the milling time it was found that this parameter varied little with t_{mill} and it remained substantially higher than the value obtained for the amorphous ribbon (482 K). This is true even for the powder milled for 100 h and indicates that this sample is far from being amorphous despite of the signatures present in the XRD and in the DSC data. Thus, the Curie temperature showed to be a parameter which can be used to evaluate the degree of amorphosity in ferromagnetic samples. T_C, like many other magnetic parameters, is strongly influenced by the crystalline structure and more particularly by local and short range interaction and can be readily measured by TGM. The glassing and the peak of the crystallization temperatures were found to vary monotonically with the DSC heating rate while the crystallization temperature remained invariant with β. Moreover, the DSC data yielded 193 kJ/mol for the activation energy associated to the crystallization process in powder samples of the $Fe_{56}Co_7Ni_7Zr_{10}B_{20}$ alloy prepared by a milling technique.

Acknowledgements We thank L. R. S. Araújo from UFCG for helping us in the early stage of this study and to FINEP, CNPq, FACEPE e CAPES (Brazilian Agencies) for financial support.

References

1. Suryanarayana C. Mechanical alloying and milling. Prog Mater Sci. 2001;46:1–184.
2. Tanaka S, Diao Z, Sugimoto T, Narita K. Solid amorphization of Fe- and Co-based alloys and their magnetic properties. J Magn Magn Mater. 1992;112:302–4.
3. Sharma S, Vaidyanathan R, Suryanarayana C. Criterion for predicting the glass ability of alloys. Appl Phys Lett. 2007;90: 3–111915.
4. Bhatt J, Murty BS. On the conditions for the synthesis of bulk metallic glasses by mechanical alloying. J Alloys Compd. 2008;459: 135–41.
5. Liu YJ, Chang ITH. The correlation of microstructural development and thermal stability of mechanically alloyed multicomponent Fe–Co–Ni–Zr–B alloys. Acta Mater. 2002;50:2747–60.
6. Gallagher PK. Thermomagnetometry. J Therm Anal Calorim. 1997;49:33–44.
7. Leu MS, Tung IC, Chin TS. Elevated temperature initial permeability study of some ferromagnetic alloys. Mater Chem Phys. 1998;57:117–24.
8. Liu T, Chen N, Xu ZX, Ma RZ. The amorphous-to-nanocrystalline transformation in $Fe_{73.5}Cu_1Nb_3Si_{13.5}B_9$ studied by thermogravimetry analysis. J Magn Magn Mater. 1996;152:359–64.
9. González A, Bonastre J, Escoda L, Suñol JJ. Thermal analysis of Fe(Co, Ni) based alloys prepared by mechanical alloying. J Therm Anal Calorim. 2007;87:255–8.
10. Luciani G, Constantini A, Branda F, Ausanio G, Hison C, Iannoti V, Luponio C, Lanotte L. Modified thermogravimetric apparatus to measure magnetic susceptibility on-line during annealing of metastable ferromagnetic materials. J Magn Magn Mater. 2004; 272–276:2310–1.
11. Cullity BD. Elements of X-ray diffraction. 1st ed. Massachussetts: Addinson Wesley; 1956.
12. Williamson GK, Hall WH. X-ray line broadening from aluminium and wolfram. Acta Metall. 1953;1:22–31.
13. Coey JMD. Magnetism and magnetic materials. 2nd ed. Cambridge: Cambridge University Press; 2009.
14. Legendre B, Sghaier M. Curie temperature of nickel. J Therm Anal Calorim. 2011. doi:10.1007/s10973-011-1448-2.
15. Inoue A, Zhang T, Koshiba H. New bulk amorphous Fe–(Co, Ni)–M–B (M = Zr, Hf, Nb, Ta, Mo, W) alloys with good soft magnetic materials properties. J Appl Phys. 1998;83:6326–8.
16. McHenry ME, Willard MA, Laughlin DE. Amorphous and nanocrystalline materials for applications as soft magnets. Prog Mater Sci. 1999;44:291–433.
17. Kissinger HE. Reaction kinetics in differential thermal analysis. Anal Chem. 1957;29:1702–6.